JOURNAL OF CATALYSIS 145, 27–36 (1994)

Orthophosphoric Acid Interactions with Ultrastable Zeolite Y: Infrared and NMR Studies

A. Corma,[1] V. Fornés, W. Kolodziejski, and L. J. Martínez-Triguero

Instituto de Tecnología Química, U.P.V.-C.S.I.C., Universidad Politécnica de Valencia, Camino de Vera, s/n, 46071 Valencia, Spain

Received April 1, 1993; revised July 12, 1993

Interaction of H_3PO_4 with extraframework aluminum of ultrastable zeolite (USY) leads to the formation of different types of aluminum phosphates, while there is no indication of the formation of SAPO zeotype structures. The total acidity of USY slightly decreases upon the H_3PO_4 treatment, while the maximum in the distribution of acid strength is shifted to milder acidities. Dealumination of the zeolite and creation of POH sites associated with $AlPO_4$ are responsible for the modifications observed. © 1994 Academic Press, Inc.

INTRODUCTION

Zeolite Y is the active component of most of the commercial cracking catalysts. Its steam dealuminated ultrastable form (USY) contains a mesopore system capable of accommodating the reactants, and combines substantial hydrothermal stability with desirable activity and selectivity. According to X-ray diffraction, the USY catalyst retains the topology and crystallinity of the parent structure and the hydroxyl nest vacancies in the framework, which are left behind by Al removal, are mostly healed by Si incorporation (1, 2). Since the SiO_4 tetrahedra are smaller than AlO_4 tetrahedra, the cubic unit-cell parameter decreases in the course of dealumination and therefore can be related to the Si/Al ratio in the framework (3). However, the steaming of zeolite NH_4–Y not only affects the framework composition, but also fills the zeolite voids with the extracted Al which remains there as extraframework Al (EFAL). Both framework and extraframework species can be studied by various spectroscopic techniques, of which infrared spectroscopy combined with the pyridine adsorption–desorption and solid-state NMR under magic angle spinning (MAS) are the most powerful.

It is obvious for acid-catalyzed reactions that an adequate information on acidic hydroxyl groups is of paramount importance. IR spectroscopy can monitor the state, i.e., populations and acidity, of the hydroxyl groups associated with framework Al (FAL) as well as of those occurring in the extraframework species (4, 5). Moreover, IR spectroscopy can provide information on external and internal defects created in the zeolite structure during dealumination, and consequently give an idea about the extent of the defect healing caused by the Si insertion (5).

When IR is combined with the adsorption–desorption of bases such as pyridine (6) and quinoline (7), it is not only possible to distinguish between Brønsted and Lewis acid sites and to probe their acid-strength distribution, but also to characterize their accessibility to reactant molecules of different sizes.

^{29}Si MAS NMR monitors the dealumination process and, from the relative intensities of the Si(nAl) signals (n = 0–4), allows one to calculate the corresponding increase in the framework Si/Al ratio (8–12). ^{27}Al MAS NMR shows in turn different types of Al (FAL and EFAL) (8–12). Thus it was found that upon dealumination the FAL^{IV} signal loses intensity to the advantage of EFAL resonances, which grow up at 0 ($EFAL^{VI}$) and 30 ppm ($EFAL^{V}$ or $EFAL^{IV}$), and shifts from 61.6 ppm in the parent material to 54.8 ppm in the dealuminated product because of the Al removal from the second and further Al tetrahedral coordination shells. The feature at 30 ppm is probably a separate signal, since it can be selectively removed by washing the zeolite with NaOH solution (13, 14) and is relatively enhanced by ^{1}H–^{27}Al cross-polarization (CP) compared to the signal of 4-coordinated Al (15–17). The signal at 30 ppm appears very close to the position of the 5-coordinated Al signal in andalusite (18), so it was suggested (13) that it can originate from $EFAL^{V}$. Recent ^{27}Al quadrupole nutation study under fast MAS indicates that both $EFAL^{V}$ and $EFAL^{IV}$ assignments are possible (15–17) and confirms that the signal at 30 ppm is an independent resonance rather than a low-frequency component of a broad second-order quadrupolar lineshape, the high-frequency counterpart of which overlaps with the signal of FAL^{IV} (19). Furthermore, the quadru-

[1] To whom correspondence should be addressed.

0021-9517/94 $5.00

pole nutation study (15, 17) provides valuable information on two resonances which were formerly resolved in the 4-coordinated spectral region for zeolite Y dealuminated with $SiCl_4$ (20). The higher frequency signal (60 ppm (20), 62 ppm in F_2 and most intensity at $\omega_{rf}/2\pi$ in F_1 (17)) decreases, compared to the other, with increasing degree of dealumination (17, 20) and corresponds to a quadrupole coupling constant C_Q of ca. 2 MHz (17), characteristic for zeolite Na-Y (12). It follows that it has to be assigned to FAL^{IV}. The lower frequency signal (52–54 ppm (20), 56 ppm in F_2 and substantial intensity at $3\omega_{rf}/2\pi$ in F_1 (17)) corresponds to C_Q = 3.5–4 MHz (17) and has to be assigned to $EFAL^{IV}$ on the basis of relative intensity and site symmetry arguments (17, 20, 21). The latter signal probably comes from amorphous silica-alumina (14, 20), which also contributes to $EFAL^{V \text{ or } IV}$ and $EFAL^{VI}$ resonances at 30 and 0 ppm, respectively.

It has been already shown that both FAL and EFAL species play a significant role during gasoil cracking on zeolites USY (20). Therefore, it is not surprising that any modification of their concentration and properties due to chemical post-treatments seriously affects the gasoil cracking activity and selectivity (22). Recently, it has been found that a strong interaction occurs between H_3PO_4 and both framework and extraframework species of ZSM-5 and that it affects zeolite acidity and catalytic activity (23–26). This is because H_3PO_4 dealuminates the zeolite and reacts with EFAL species to form aluminum phosphate. The opinion prevails that incorporation of P atoms into the zeolite framework and Si–O–P bond formation do not occur (23, 25). However, other spectroscopic methods could be helpful to achieve more conclusive information on this matter. We note that all the preliminary solid-state NMR work on P-impregnated ZSM-5 (23–26) indicates clearly that by an adequate H_3PO_4 treatment it should be possible to modify the physicochemical characteristics of zeolite USY, and consequently the cracking activity.

In our work a series of H_3PO_4-impregnated USY zeolites containing various amounts of P and treated under various thermal conditions have been jointly studied by IR spectroscopy combined with the pyridine adsorption-desorption, by thermoprogrammed desorption of ammonia (TPDA), and by ^{29}Si, ^{27}Al, and ^{31}P solid-state MAS NMR.

EXPERIMENTAL

Zeolite USY was prepared from zeolite NH_4Y (Si/Al ratio of 2.7) by 5 h steaming at 823 K. This sample was then impregnated with H_3PO_4 solution to obtain zeolites with 0.5, 1, 2, 4, and 6 wt% of P, which were next calcined for 1 h at 773 K (P0 samples). A second series of the USY samples was obtained by steaming the P0 samples during 5 h at 1023 K (PS samples). Table 1 collects the physicochemical characteristics of all the samples studied.

TABLE 1

Physicochemical Characteristics of USY Samples

Sample	a_0 (nm)	Cryst.[a] (%)	Si/Al (XRD)	Si/Al (NMR)
USY000	2.448	95	5.9	5.4
USY05P0	2.448	96	5.9	—
USY1P0	2.443	96	7.7	7.9
USY2P0	2.443	95	7.6	—
USY4P0	2.440	81	9.2	7.3
USY6P0	—	22	—	12.7
USY00S	2.428	91	35	—
USY05PS	2.428	89	35	—
USY1PS	2.428	84	35	—
USY2PS	2.428	85	35	—
USY4PS	2.428	80	35	—
USY6PS	—	21	—	—

[a] The crystallinity was calculated by comparing the peak height of the (5, 3, 3) reflection and considering YNa (LZY-52) to be 100% crystalline.

IR experiments were performed using vacuum cells. Wafers of 10 mg cm^{-2} were degassed overnight under vacuum (10^{-3} Pa) at 673 K. The spectra were recorded and then pyridine (6×10^2 Pa) was admitted and, after equilibration, desorbed for 1 h at increasing temperatures (523 K/623 K/673 K). After each desorption step the spectra were recorded at room temperature.

The TPD of ammonia from USY samples (0.1 g) was carried out in a stream of He (100 ml min^{-1}) with a heating rate of 10 K min^{-1}. Prior to the TPDA experiments the samples were activated at 723 K for 2 h in a stream of O_2 (50 ml min^{-1}). Ammonia adsorption was carried out at 450 K in order to eliminate the physically adsorbed NH_3, and the amount desorbed was detected using a TCD device and determined from the area of the desorption peak.

Solid-state ^{31}P, ^{27}Al, and ^{29}Si NMR spectra were recorded under magic angle spinning (MAS) at ambient temperature on a Varian Unity VXR-400 WB spectrometer at 161.9, 104.2, and 79.5 MHz, respectively. For ^{31}P and ^{29}Si both the conventional Bloch decay (BD) and cross-polarization (CP) spectra were measured. A high-speed MAS Doty probe with zirconia rotors (5 mm in diameter) was used for ^{31}P NMR and a Varian MAS probe with zirconia rotors (7 mm in diameter) was used for ^{27}Al and ^{29}Si NMR. The acquisition parameters are given in Table 2. The MAS rotors were driven by dry air and the magic angle was set precisely by observing the ^{79}Br resonance of KBr. The CP spectra were recorded with single contacts and the contact times were optimized on the original samples. ^{29}Si spectra were deconvoluted with standard Varian software and the

TABLE 2

MAS and CP/MAS NMR Acquisition Parameters

Resonance	Pulse (μs)	MAS Flip angle (radians)	Recycle delay (s)	MAS rate (kHz)
^{31}P	3.0	$(3/8)\pi$	15	7.0–7.3
^{27}Al	0.6	$\pi/20$	0.5	8.5
^{29}Si	4.0	$\pi/5$	40	6.0

Resonance	$\pi/2$ Pulse (μs)	CP/MAS Contact time (ms)	Recycle delay (s)	MAS rate (kHz)
^{31}P	5.5	1.5	3	6.5
^{29}Si	9.0	3.0	2	5.0

$(Si/Al)_{NMR}$ ratios were calculated from the peak areas using the classic equation given in the literature (8–12).

RESULTS AND DISCUSSION

Infrared and Temperature-Programmed Desorption

IR spectroscopy (Fig. 1, a1) detects various kinds of hydroxyl groups in the USY zeolite (4). Bridging hydroxyl groups from the zeolite framework (conventional Brönsted sites) give bands at 3632 and 3559 cm^{-1}, so hereafter are refered to as the high frequency (HF) and low frequency (LF) hydroxyls, respectively. The bands at 3600 and 3525 cm^{-1} are assigned to the HF and LF framework hydroxyls, respectively, interacting with EFAL species. Because of this interaction the hydroxyl groups become more acidic (superacid sites) and the corresponding bands are shifted to the lower frequences. Hydroxylated EFAL species are responsible for the 3670 cm^{-1} (pseudobohemite) and 3600 cm^{-1} bands, the latter being a background for all four bridging hydroxyl bands. The highest frequency band at 3746 cm^{-1} has been assigned to external silanol groups.

After the pyridine adsorption (Fig. 1, a2) all the accessible acidic hydroxyls disappeared, while the nonacidic hydroxyls, i.e., the external silanols (the band at 3746 cm^{-1}) and the hydroxylated EFAL species (the bands at 3700 and 3600 cm^{-1}), remained unreacted (4).

Upon P-incorporation (1–4 wt%) the intensity of the hydroxyl bands decreased (Fig. 2) and so did the Brønsted and Lewis acidity measured by the pyridine adsorption (Table 3). This can be a result of zeolite dealumination by the H_3PO_4 treatment, in accordance with the contraction of the zeolite unit cell (Table 1). Furthermore, the decreased intensity of the EFAL hydroxyl band at 3600 cm^{-1} as well as the effect on the Lewis acidity (Table 3) would indicate strong interaction of H_3PO_4 with the EFAL species, leading probably to the aluminum phosphate formation (IR results for the steamed samples, vide infra). The effects for the USY4P0 sample are particularly notable (Fig. 2c).

The NH_3 TPD technique monitors the acid strength distribution. Our results (Fig. 3) show that the H_3PO_4 treatment preferentially removes the strong acid sites (635 K) while increasing the amount of those with the medium-low acidity (535 K). We submit that the dealumination alone would decrease the total amount of the acid sites and increase a fraction of the stronger Brönsted acid sites. It turns out that H_3PO_4 is not only a dealuminating agent.

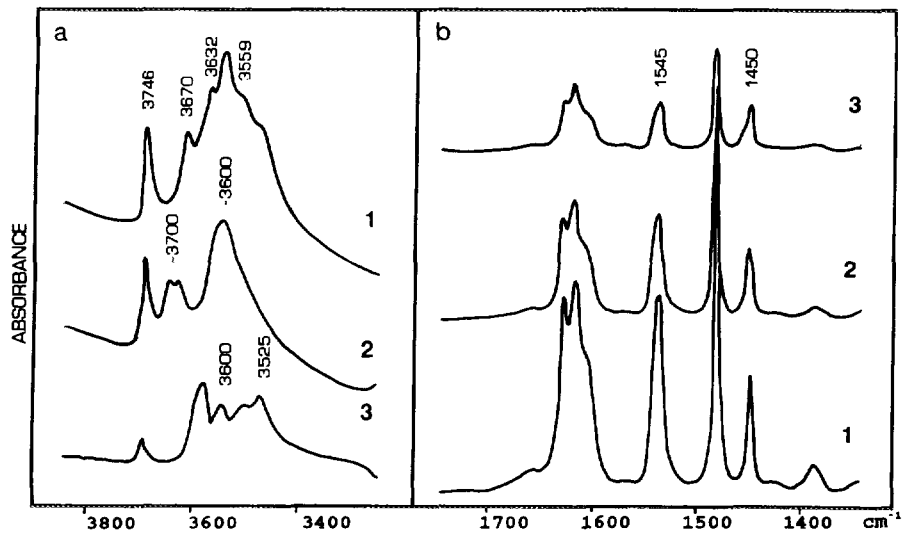

FIG. 1. IR spectra of the USY000 sample. (a) Hydroxyl range (1) before and (2) after pyridine adsorption, and (3) difference spectrum. (b) Spectra of pyridine adsorbed at room temperature and desorbed at (1) 523 K, (2) 623 K, and (3) 673 K.

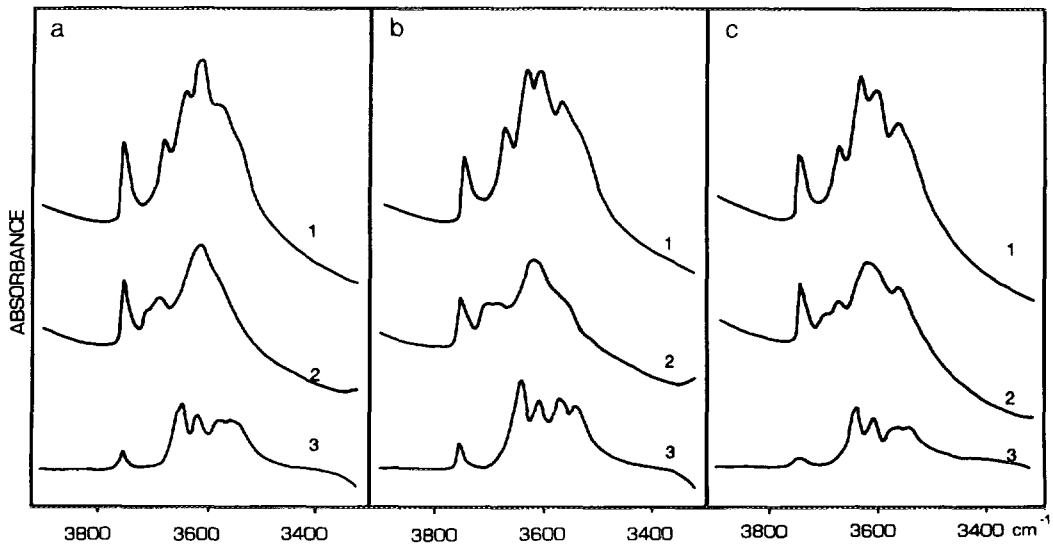

FIG. 2. IR spectra in the hydroxyl range of (a) USY1P0, (b) USY2P0, and (c) USY4P0. The same legend for (1), (2), and (3) as in Fig. 1.

The shift towards the milder acidity could be explained by preferential interaction of P-containing species with the strong acid sites, and/or by their interaction with this EFAL, which induces the superacid hydroxyls having the IR bands at 3600 and 3525 cm^{-1}. However, the IR results in the OH region (cf. Fig. 1 and 2) do not support the latter conclusion because the P-impregnation and subsequent calcination hardly affect the superacid hydroxyl bands. We believe that the H_3PO_4 treatment creates some acid sites of medium and low acid strength, probably POH groups, if the aluminum phosphate formation is assumed. According to the molecular orbital calculations (27, 28), such POH groups have acidic properties and are quite stable. Moreover, AlOH groups can enhance the POH acidity by hydrogen bonding (29). On top of this, the presence of bridged P–OH–Al hydroxyl groups, which are more acidic than the POH groups, cannot be ruled out.

Upon steaming the intensity of the hydroxyl bands dramatically decreased (Fig. 4) and only the silanol band and a band at 3680 cm^{-1} have been detected. The latter, well visible for USY4PS (Fig. 4c), comes from the POH groups, thus suggesting the presence of the aluminum phosphate species. As concerns the acidity measured by the pyridine adsorption, a maximum in the total (Brønsted and Lewis) acidity was found for the sample containing 1 wt% of P (Table 3), and all the samples reached the same final unit-cell size despite the different P-contents (Table 1).

TABLE 3

Brønsted and Lewis Acidity of the USY Samples as a Function of the Degassing Temperature (Values in μmol g^{-1} of Pyridine Adsorbed)

	Brønsted			Lewis		
Sample	523 K	623 K	673 K	523 K	623 K	673 K
USY000	192	109	49	52	34	23
USY1P0	115	60	27	29	29	23
USY2P0	137	60	27	42	29	29
USY4P0	93	71	33	16	23	23
USY6P0	42	21	4	19	15	12
USY00S	2	<1	<1	6	2	2
USY1PS	2	1	<1	13	4	4
USY2PS	2	1	<1	12	4	4
USY4PS	1	<1	<1	8	3	2
USY6PS	<1	<1	<1	4	1	<1

Solid-State NMR

Our ^{29}Si MAS NMR spectra (Fig. 5) show that the impregnation of USY with H_3PO_4 dealuminates the zeolite. This is reflected in the framework Si/Al ratios obtained by deconvolutions of the NMR patterns, which data reasonably agree with those deduced from the unit-cell size (Table 1). Upon steaming a more severe dealumination occurs since the ^{29}Si BD spectra show only a peak of Si(0Al) (8, 12). We have also found a background signal from silica (30, 31) (e.g., see the USY6PS spectrum in Fig. 5) having in a series of samples an average chemical shift of -111.9 ppm (the deconvolution results).

There is no indication of any isomorphous substitution of framework Si by P during steaming and any formation of the corresponding P–O–Al–O–Si bonds, at least to the NMR detectable extent, because a signal at ca. -90 ppm characteristic for SAPO-37 (32) which is isostructural with

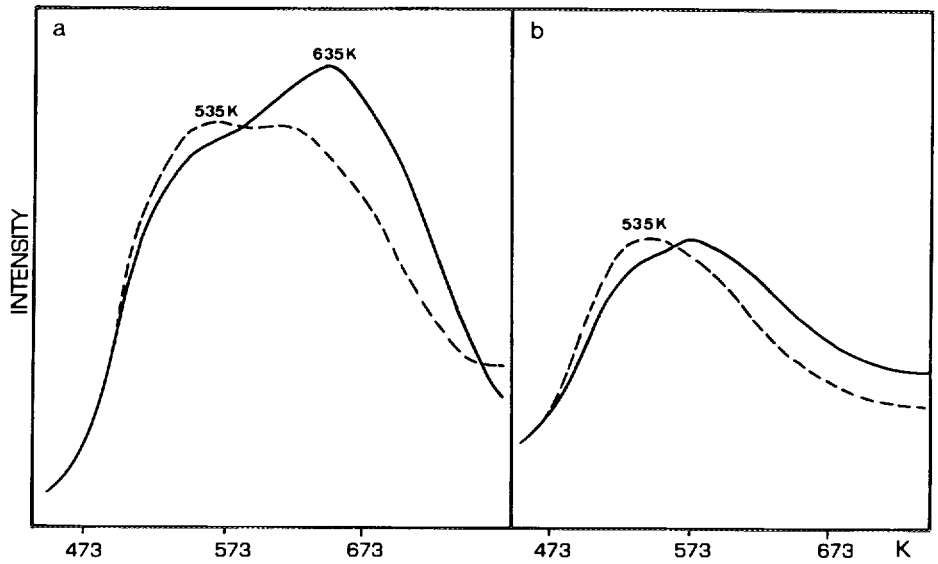

FIG. 3. Thermoprogrammed ammonia desorption profiles for the USY samples before (—) and after (---) H_3PO_4 adsorption (1 wt% P). (a) nonsteamed and (b) steamed.

faujasite, is absent in our spectra of the P-impregnated samples.

Signal positions in the conventional ^{27}Al spectra are not usually very characteristic because they are not only dependent on chemical shifts but also on quadrupolar parameters of the respective Al sites. However, we have observed several typical features (Fig. 6). Thus there are FAL^{IV}, $EFAL^{IVorV}$, and $EFAL^{VI}$ resonances at 56–58, 30, and at −3 to 4 ppm, respectively, coming from the part of the material, which has not been affected by the P-impregnation (Fig. 6). These can be easily identified for the samples without P or those with the low P-content (0.5 and 1%). Then we note that the spectrum of USY4PS (Fig. 6) is almost identical with the spectrum of sample APAl-A (Fig. 3 in Ref. (33)) containing amorphous system $AlPO_4$–Al_2O_3 (75 : 25 wt%). It follows that the signals from USY4PS at 37 ppm ($EFAL^{IV}$) and at −6 ppm ($EFAL^{VI}$) can be assigned to the similar extraframework material. The position of 4-coordinated Al signal from the amorphous $AlPO_4$–Al_2O_3 phase shows up for the nonsteamed sample at 44 ppm (USY4P0), while for the steamed material it is located at 37 ppm (USY4PS), perhaps because

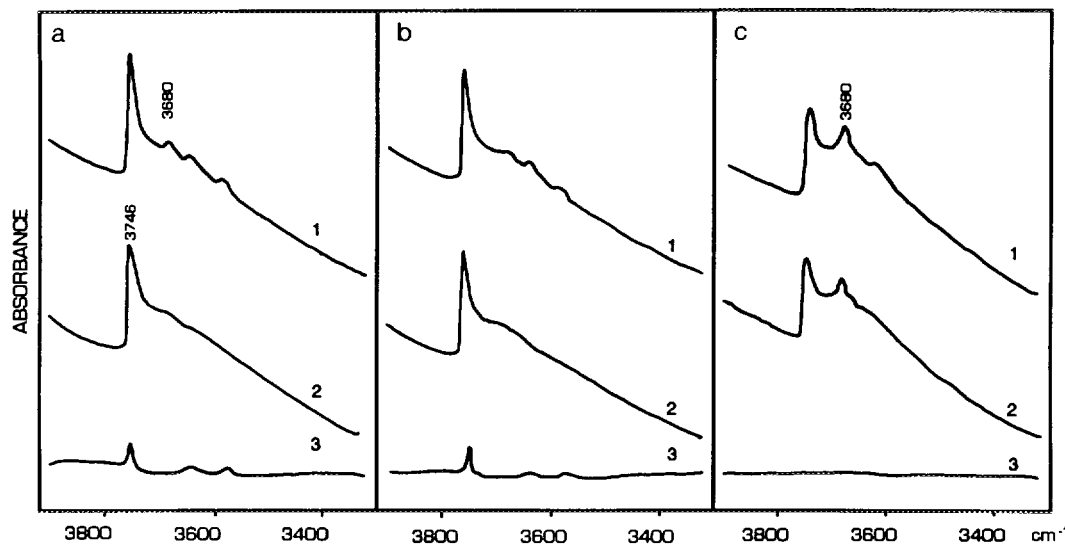

FIG. 4. IR spectra in the hydroxyl range of (a) USY1PS, (b) USY2PS, and (c) USY4PS. The same legend for (1), (2), and (3) as in Fig. 1.

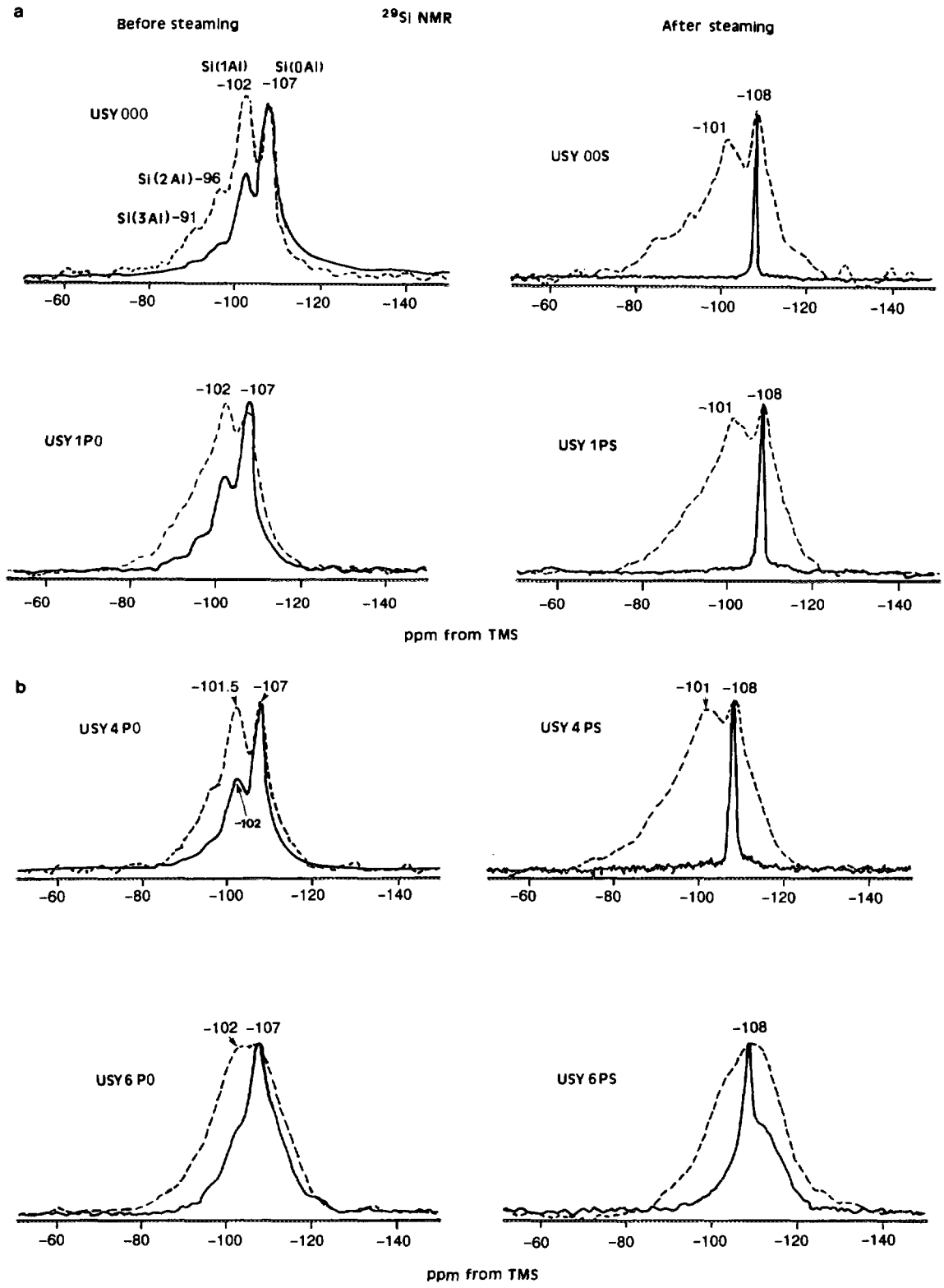

FIG. 5. ^{29}Si NMR Bloch decay (full line) and cross-polarization (dashed line) spectra of ultrastable zeolite Y modified with H_3PO_4.

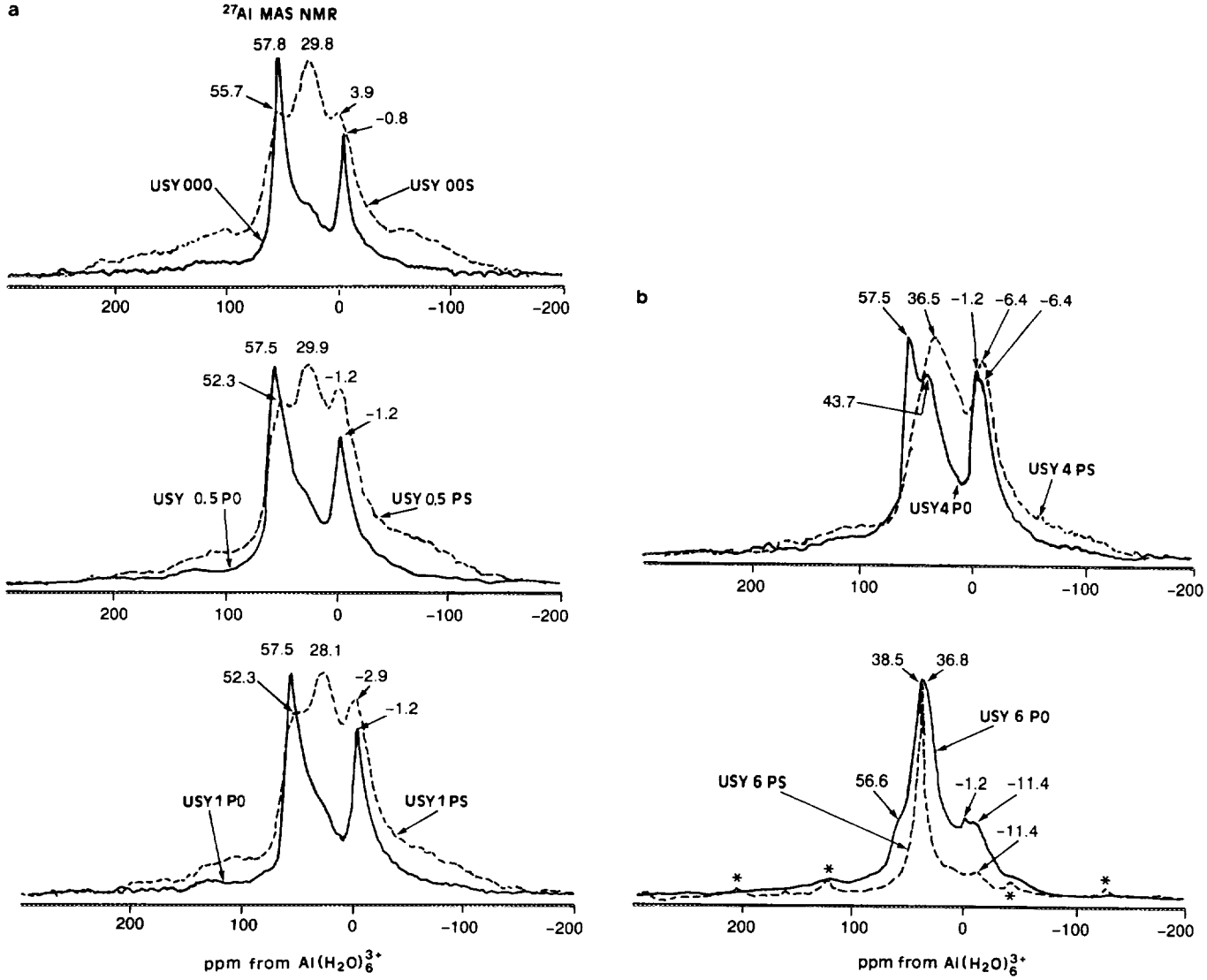

FIG. 6. ^{27}Al NMR Bloch decay spectra of ultrastable zeolite Y modified with H_3PO_4. Full and dashed lines denote nonsteamed and steamed samples, respectively. Asterisks denote spinning sidebands.

of its different Al_2O_3 content. We also assume this signal to be present in the spectra of the nonsteamed samples with the low P-content, since the 4-coordinated Al signal gradually broadens from USY000 to USY1P0, before it finally separates for USY4P0. For the steamed samples with the low P-content (USY05PS and USY1PS) the 4-coordinated Al signal from the amorphous $AlPO_4$–Al_2O_3 phase is perhaps strongly overlapped with the FAL^{IV} signal of nonmodified USY, so the joint signal has a maximum at ca. 52 ppm. In order to clarify the problem of the superimposed Al resonances we plan to do quadrupole nutation experiments.

For USY6P0 (Fig. 6) there are some minor peaks of nonmodified USY at 57 and -1 ppm and the predominant peaks at 37 and -11 ppm, characteristic for amorphous aluminum phosphate (33). Hydrothermal treatment of this sample results in substantial narrowing and shift from 36.8 to 38.5 ppm of the 4-coordinated Al signal and almost elimination of the 6-coordinated Al signal at -11.4 ppm (cf. USY6P0 and USY6PS in Fig. 6e). The signal positions and the spectral effects are the same as observed by Sanz *et al.* (33) during crystallization of amorphous aluminum orthophosphates. It follows that the sharp 4-coordinated Al signal of USY6PS has to be assigned to crystalline $AlPO_4$.

However, our NMR results reflect only averaged phenomena, that is they cannot distinguish between $AlPO_4$ in an outer shell of zeolite crystals and that deposited in internal voids. Therefore, no comment can be done on a gradient in the $AlPO_4$ concentration over individual zeolite crystals

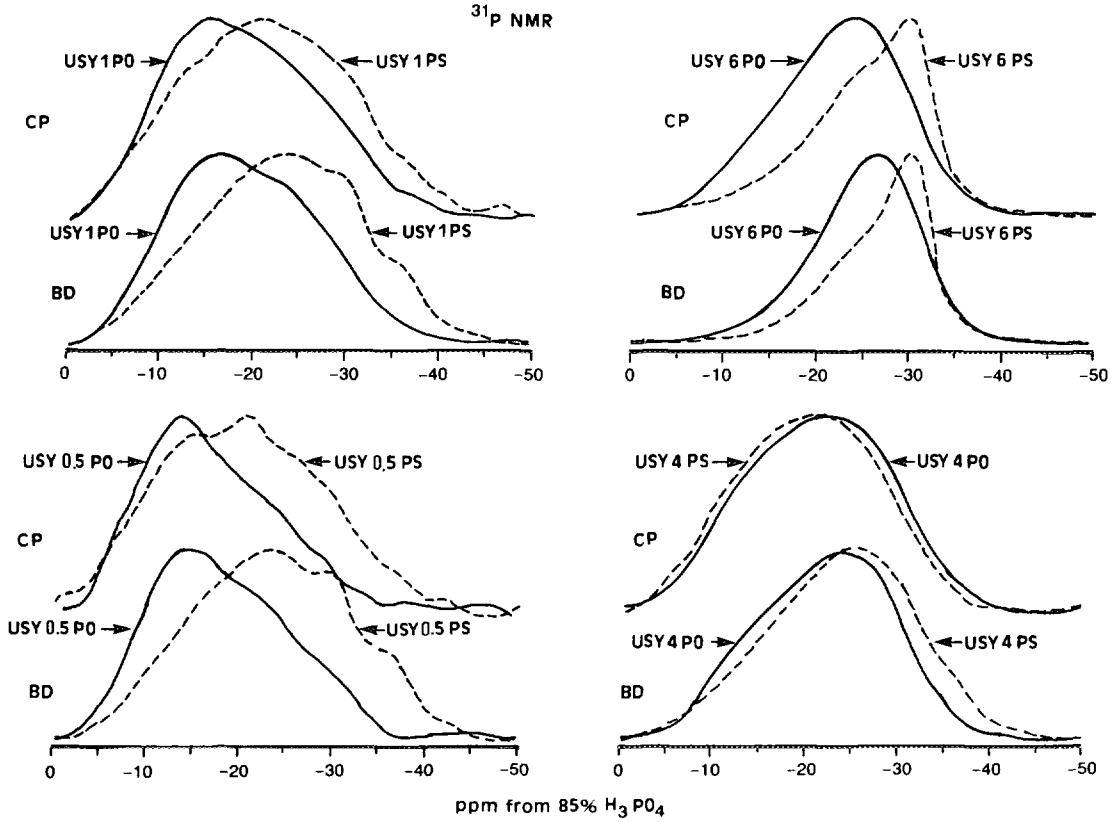

FIG. 7. ^{31}P NMR Bloch decay (BD) and cross-polarization (CP) spectra of ultrastable zeolite Y modified with H_3PO_4. Full and dashed lines denote nonsteamed and steamed samples, respectively.

(23). However, we checked that the crystallization of $AlPO_4$ substantially decreases the BET surface area from 335 to 123 $m^2 g^{-1}$ and causes an increase of silica content by a factor of 2.6 (our ^{29}Si NMR results). The former effect suggests that crystalline $AlPO_4$ is formed at the crystal surface of zeolite, the latter that the process occurs also inside the framework resulting in its partial destruction.

^{31}P NMR brings a further evidence of $AlPO_4$ formation during the H_3PO_4 interaction with USY (Fig. 7). Consider BD spectra. Amorphous $AlPO_4$ gives one broad signal at -26 ppm (cf. USY6P0) (33). After hydrothermal treatment a sharper signal arises at -30 ppm (cf. USY6PS), which can be assigned to crystalline $AlPO_4$ (tridymite structure) (33). Accordingly, we suggest that USY4P0 and USY4PS contain P mainly in the form of amorphous $AlPO_4$ (broad BD signals with the maxima at -23.5 and -25 ppm, respectively). For the low P-content there are two extra signals: at ca. -15 ppm of short chain polyphosphates (34), which decreases after steaming, and one at ca. -37 ppm of highly condensed polyphosphates (35), which appears after steaming. Note that the spectra in Fig. 7 are not in the absolute intensity mode, but all are scaled to the same arbitrary amplitude. In reality, the samples with the higher P-content give more intense spectra. The polyphosphate signal is better resolved for the samples with the low P-content but is certainly bigger, although more superimposed on neighbor signals, in the samples with the high P-content. All the ^{31}P signals are considerably overlapped but it is evident that the $AlPO_4$ signals increase upon steaming.

In order to discuss the formation of mild acid sites associated with POH groups we refer to the ^{31}P CP spectra. CP favors higher frequency signals (Fig. 7), which is also proved by the variable contact-time experiment (Fig. 8). For the short contact time (100 μs) species containing protons are preferred and they give continuous absorption roughly in the -10 to -22 ppm range. Just in this range a wide POH signal from the amorphous phase has been detected (36), so our short contact time spectrum suggests that in the P-containing samples there is a wide distribution of POH sites residing in chemically varying and ill defined environments. These hydroxyls are of medium and weak acidity (37), and can affect the acid strength distribution observed in the H_3PO_4 treated USY samples.

CONCLUSIONS

On the basis of the IR, TPDA, and NMR results we

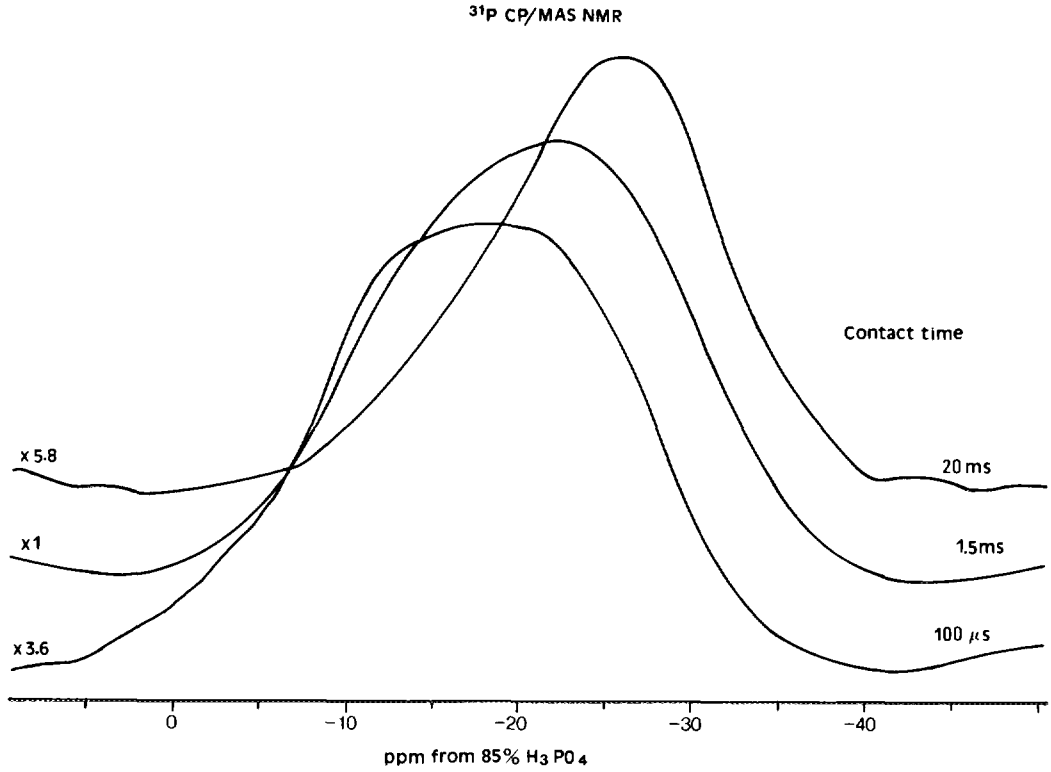

FIG. 8. ^{31}P NMR variable contact-time CP spectra of sample USY4P. Note various intensity scaling factors given in the figure.

conclude that H_3PO_4 dealuminates the USY framework and interacts strongly with the EFAL species to give amorphous $AlPO_4$–Al_2O_3 phase, whose composition depends on the treatment conditions. The interaction increases with the H_3PO_4 concentration and upon steaming, and some $AlPO_4$ crystallizes in the tridymite structure. The H_3PO_4 treatment causes dealumination of USY, thus decreasing the total number of Brønsted acid sites and the area below the TPDA curve at higher temperatures. At the same time the H_3PO_4 treatment produces new milder acid sites, that is POH groups, which are responsible for the increase in the area below the TPDA curve at lower temperatures. The overall effect results in a shift of the acid strength distribution towards milder acidities.

ACKNOWLEDGMENTS

Financial support by CICYT (Project MAT 91-1152) is gratefully acknowledged. W.K. thanks the Spanish Ministry of Education for Grant SB92-A00751599.

REFERENCES

1. McDaniel, C. V., and Maher, P. K., "Molecular Sieves," p. 186. Society of Chemical Industry, London, 1968; McDaniel, C. V., and Maher, P. K., U.S. Patent 3,449,070 (1969).
2. McDaniel, C. V., and Maher, P. K., "Zeolite Chemistry and Catalysis," ACS Monograph, Vol. 171, p. 285. Am. Chem. Soc., Washington, DC, 1976; Breck, D. W., "Zeolite Molecular Sieves: Structure Chemistry and Use." Wiley, New York, 1974.
3. Fichtner-Schmittler, H., Lohse, U., Engelhardt, G., and Paizelova, V., *Cryst. Res. Technol.* **19,** K1 (1984).
4. Corma, A., Fornés, V., and Rey, F., *Appl. Catal.* **59,** 267 (1990).
5. Barthomeuf, D., *in* "Zeolite Microporous Solids: Synthesis, Structure and Reactivity" (E. G. Derouane, F. Lemos, C. Naccache, and F. R. Ribeiro, Eds.), NATO ASI Series, Vol. 352, p. 193. Kluwer, London, 1992.
6. Corma, A., Fornés, V., Martinez, A., and Orchillés, A. V., *in* "Perspectives in Molecular Sieve Science" (W. H. Flank and T. E. Whyte, Eds.), ACS Symposium Series, Vol. 368, p. 542. Am. Chem. Soc., Washington, DC, 1988.
7. Corma, A., Fornés, V., and Rey, F., *Zeolites* **13,** 56 (1993).
8. Klinowski, J., *Prog. NMR Spectrosc.* **16,** 237 (1984).
9. Klinowski, J., *Annu. Rev. Mater. Sci.* **18,** 189 (1988).
10. Klinowski, J., *Colloids Surf.* **36,** 133 (1989).
11. Klinowski, J., *Chem. Rev.* **91,** 1459 (1991).
12. Engelhard, G., and Michel, D., "High Resolution Solid-State NMR of Silicates and Zeolites." Wiley, New York, 1987.
13. Gilson, J. P., Edwards, G. C., Peters, A. W., Rajagopalan, K., Wormsbecher, R. F., Roberie, T. G., and Schatlock, M. P., *J. Chem. Soc. Chem. Commun.*, 91 (1987).
14. Corma, A., Fornés, V., Martinez, A., and Sanz, J., *in* "Fluid Catalytic Cracking Role in Modern Refining" (M. L. Ocelli, Ed.), ACS Symp. Ser. Vol. 375, p. 17. Am. Chem. Soc., Washington, DC, 1988.
15. Rocha, J., and Klinowski, J., *J. Chem. Soc. Chem. Commun.*, 1121 (1991).
16. Rocha, J., and Klinowski, J., *in* "Molecular Sieves, Synthesis of

Microporous Materials" (M. L. Ocelli and H. E. Robson, Eds.), Vol. I, p. 71. Van Nostrand–Reinhold, New York, 1992.
17. Rocha, J., and Klinowski, J., *Chem. Phys. Lett.* **187,** 401 (1991).
18. Lippmaa, E., Samoson, A., and Mägi, M., *J. Am. Chem. Soc.* **108,** 1730 (1986).
19. Samoson, A., Lippmaa, E., Engelhardt, G., Lohse, U., and Jerschkewitz, H. G., *Chem. Phys. Lett.* **134,** 589 (1987).
20. Sanz, J., Fornés, V., and Corma, A., *J. Chem. Soc. Faraday Trans. 1* **84,** 3113 (1988).
21. Ray, G. J., Meyers, B. L., and Marshall, C. L., *Zeolites* **7,** 307 (1987).
22. Chitnis, G. K., and Herbst, J. A., U.S. Patent 5,110,776 (1992), and references therein.
23. (a) Caro, J., Bülow, M., Derewinski, M., Hunger, M., Kärger, J., Kürschner, U., Pfeifer, H., Storek, W., and Zibrowius, B., *Stud. Surf. Sci. Catal.* **52,** 295 (1989); (b) Caro, J., Bülow, M., Derewinski, M., Haber, J., Hunger, M., Kärger, J., Pfeifer, H., Storek, W., and Zibrowius, B., *J. Catal.* **124,** 367 (1990).
24. Öhlmann, G., Jerschkewitz, H. G., Lischke, G., Eckelt, R., Parlitz, B., Schreier, E., Zibrowius, B., and Löffler, E., *Stud. Surf. Sci. Catal.* **65,** 1 (1991).
25. Lischke, G., Eckelt, R., Jerschkewitz, H. G., Parlitz, B., Schreier, E., Storek, W., Zibrowius, B., and Öhlmann, G., *J. Catal.* **132,** 229 (1991).
26. Reschetilowski, W., Einicke, W. D., Meier, B., Brunner, E., and Ernst, H., *in* "Zeolite Chemistry and Catalysts" (P. A. Jacobs *et al.*, Eds.), p. 119. Elsevier, Amsterdam, 1991.
27. Pelmenshchikov, A. G., and Zhidomirov, G. M., *React. Kinet. Catal. Lett.* **23,** 295 (1983).
28. Zhidomirov, G. M. and Kazansky, V. B., *Adv. Catal.* **34,** 131 (1986).
29. Moffat, J. B., Vetrivel, R., and Viswanathan, B., *J. Mol. Catal.* **30,** 171 (1985).
30. Fyfe, C. A., Gobbi, G. C., and Kennedy, G. J., *J. Phys. Chem.* **30,** 277 (1985).
31. Anderson, M. W., and Klinowski, J., *J. Chem. Soc. Faraday Trans. 1* **82,** 1449 (1986).
32. Saldarriaga, L. S., Saldarriaga, C., and Davies, M. E., *J. Am. Chem. Soc.* **109,** 2886 (1987).
33. Sanz, J., Campelo, J. M., and Marinas, J. M., *J. Catal.* **130,** 642 (1991).
34. Grimmer, A. R., and Haubenreisser, T., *Chem. Phys. Lett.* **99,** 487 (1983).
35. Duncan, T. M., and Douglas, D. C., *Chem. Phys.* **87,** 339 (1984).
36. Kolodziejski, W., He, H., and Klinowski, J., *Chem. Phys. Lett.* **191,** 117 (1992).
37. Yoshida, N., Kimvra, T., Sugimoto, M., Nishida, M., Ogawa, H., and Kishimoto, S., *J. Catal.* **139,** 568 (1993).